

Reduced model for the description of radiation-matter interaction including atomic recoil

J. Javaloyes and G. L. Lippi

Institut Non Linéaire de Nice, UMR 6618 CNRS, Université de Nice–Sophia Antipolis, 1361 Route des Lucioles, F-06560 Valbonne, France

A. Politi

Istituto Nazionale di Ottica Applicata, Largo E. Fermi 6, 50125 Firenze, Italy

(Received 15 January 2003; published 12 September 2003)

We show that a model for the collective atomic recoil laser, previously introduced to include collisions with an external buffer gas, can be reduced to a single dynamical equation for the probe amplitude. This is the result of a clever adiabatic elimination of the atomic variables and of the assumption of a negligible effect of the probe field onto the atomic motion. This reduced model provides a fairly accurate description of the phase diagram of the original set of equations and allows for the investigation of more realistic regimes, where the direct simulation of the full model would be otherwise unfeasible. As a result, we find that the onset of a coherent field can be either described by a second- or first-order transition, the former scenario being observable only below a given temperature. Moreover, the first-order transition is accompanied by an intrinsic optical bistability region.

DOI: 10.1103/PhysRevA.68.033405

PACS number(s): 42.50.Vk, 05.45.Xt, 05.65.+b, 42.65.Sf

I. INTRODUCTION

The interaction between atoms and the electromagnetic (e.m.) radiation is a domain of physics that has attracted attention for over a century. At the origin of the development of quantum mechanics, the interpretation of atomic (and molecular) spectra and the prediction of their features has been the object of a large wealth of work (e.g., cf. Refs. [1–5]). The problem has been analyzed, in most cases, semiclassically, but fully quantum mechanical treatments have been also carried out. Within the semiclassical approach—the scope of the present work—several authors have developed ways of treating the interaction between a quantized two-level (or multilevel) atom, with a formalism analogous to the vector description of spin states [6], and the classical (macroscopic) e.m. field. This way of modeling the interaction is particularly appealing when the e.m. field is sufficiently strong to neglect its fluctuations, and whenever the atomic response to the external field is sought. The number of physical effects that can be treated in this fashion is particularly large, and the complete literature cannot be cited here (a good overview of a number of classic effects can be found in Refs. [7,8]). Within this framework, the contribution of this paper is to take into account aspects that so far have been treated independently or in a perturbative approach: the effect of the radiation scattered by the atoms into the global e.m. field and its feedback on the atoms [9], i.e., taking into account the atomic motion due to atomic recoil (because of the photon exchange) and collisions (between atoms).

The rest of this introduction is dedicated to a brief review of known effects that are going to play a role in the system we choose to describe. Some of them will be arbitrarily excluded (e.g., Rayleigh or Raman scattering) from our discussion, but they are indeed contained in the literature cited, as well as in the problem that we consider and in the way we treat it.

The advent of the laser marked a revolution in the study

of light-atom interactions. Work concerning the shape of atomic emission spectra under different experimental conditions was published very early on [10–12] and applications to nonlinear effects arising in gas laser amplifiers were considered [13,14]. In Refs. [10–12] it was also shown that, at the lowest level of semiclassical description, the study of the response of a two-level atom to the incident radiation requires the inclusion of saturation effects on the optical transition and the influence of detuning between field and atoms. Immediately, a concern arises about the strength of the incident radiation, which modifies the atom's level structure, introducing the so-called Rabi sidebands (or level splitting) [15]: the absorption and emission spectrum of the atom have been strongly modified by the interaction. The development of narrow-linewidth and sufficiently powerful tunable lasers allowed for experimentally probing, a few years later, these somewhat surprising predictions. The experiments [16–19] confirmed the existence of sidebands—an object of debate, at the time—but also showed that the complete picture was quite more complex.

One of the questions that presented themselves concerned the measurement of the modifications in the atomic spectral properties when subject to an intense external field. For this purpose, it was natural to introduce a second field of variable frequency and of very weak intensity, which may be scanned across the frequency range over which the atom reacts, without perturbing in any significant way the atomic line shape: a weak *probe* field. Unfortunately, the mathematical treatment of the problem becomes immediately intractable in closed form, and approximations have to be introduced [20].

The problem of two independent traveling waves (pump and weak probe) interacting with an atomic sample was first investigated in the 1960s with reference to a multilevel atomic structure [11,21–23] and a detailed discussion can be found already in Ref. [24]. A subsequent, more general, treatment of the interaction of an ensemble of atoms with quasisonant counterpropagating pump and probe fields, includ-

ing their spatial dependence and the transition's Doppler broadening, has become a standard reference [25]. There, the interaction between pump field and atoms is calculated exactly, while the probe's evolution is treated in a perturbative form. Integration over the Doppler velocity distribution is included. As a result, detailed spectral features, consisting of attenuation and amplification peaks for the probe field, were found (also function of the atomic speed). More significantly, in Ref. [25] it was proven that atomic motion can hardly be neglected in the treatment of these problems.

The first consequence of motion in thermal atomic samples is to shift the individual atom's resonance frequency by a certain amount (Doppler shift). A thermal sample will therefore behave with an integrated response, weighted over the various velocity population classes, of atoms seeing both pump and probe shifted by different amounts (relative to the atomic resonance). The result of the Doppler integration (or broadening) is not simply that of smoothing out the profiles, but, rather, that of introducing velocity-selective effects which give rise to spectral dips (or holes) [26–30], hole burning [31], so-called “dead zones” [32]—i.e., frequency intervals for which the global atomic susceptibility for the sample is nearly nonexistent—, and various other features that have been discussed in numerous publications (e.g., without [33] or with [34] Doppler broadening). The effects of relative directionality between pump and probe have also been carefully investigated and have been shown to induce different spectral signatures [35,36]. Additional features present in the interaction between atoms and two fields are the excitation of harmonics in the combination of field's frequencies (e.g., with cross-polarized fields [37]) or washout effects of the grating in the atomic variables imposed by the periodic modulation coming from the interference between fields [31,38]. The latter paper introduces a formalism that allows for the treatment of several different kinds of problems and nonlinearities, taking into account also the nonlocality of the interaction and washout effects of spatial structures due to atomic motion.

Motion does not only influence the shape of the atomic response through Doppler shift or washout of gratings, but also gives rise to more subtle phenomena. If one considers the momentum transfer between atoms and field, due to the exchange of photons, then the atomic velocity becomes itself a variable in the problem. One might be tempted to say that such effects become important only for cold atoms; in such a case, resonances can be shifted or modified by the recoil transfer (e.g., Refs. [39,40]). Particular features in the resonances have been observed in pump-probe experiments using very cold atoms [41], but the possibility of obtaining gain from a two-level system, due to the change in atomic momentum during the interaction and in the absence of any population inversion, was predicted very early on [42], and was later investigated in detail (e.g., Refs. [43,44]). However, the transfer of momentum between atoms and the e.m. field is not restricted to cold atomic samples. Atomic beams have been shown to display resonances [45,46] that couple the internal atomic degrees of freedom to the external motion: dopplerons [47–50]. Momentum transfer, i.e., a change in atomic momentum, is equivalent to forces that act on the

atoms. Such forces have played a crucial role in atomic cooling with lasers [51], but are generally present in all problems (cf., e.g., Ref. [52]). Indeed, their action is responsible for the predicted appearance of coherent lasing action through atomic bunching (the collective atomic recoil laser, or CARL, Ref. [53]) or through other collective effects [54,55]. The existing experimental evidence for CARL has been the object of debate [56,57], but a collective behavior (perhaps the one of Ref. [54]) may be at the origin of some anomalous gain [58,59] which appears only for particularly strong pump values, and not under the conditions for which usual pump-probe spectroscopy experiments are conducted (e.g., Ref. [60]).

In any case, precision measurements show that recoil plays a role in pump-probe spectroscopy even when collective effects are not relevant. The originally measured spectra [16,17,19] present features that are typical of recoil and the spectral details could not be explained until the latter was taken into account [61,62]. This is a clear indication that the transfer of momentum between e.m. field and atoms is not entirely negligible even when thermal (hot) atomic samples are considered. It is therefore reasonable that recoil should also lead to new features such as collective behavior.

One further consequence of atomic motion, and of momentum transfer, is the change in velocity that the atoms undergo during the interaction. For weak coupling, it is reasonable to expect that the modifications in the velocity distributions remain small and that the thermal profile dominates, but if the coupling is strong, substantially different shapes for the momentum distribution may appear [45–47,55]. These effects are important not only for a basic understanding of the medium's internal dynamics, but have been used for preparing samples with particular velocity distributions (e.g., Refs. [63,64]).

Often, a buffer gas is added to the atomic vapor, either to change the type of broadening in a hot vapor [65], or for purely technical reasons—such as keeping the vapor away from the optical windows—, or both. Either way, neglecting collisions is often impossible, and their role has to be taken into account. For our purposes, we will ignore collisions with the walls of the container, and concentrate, instead, on two-body interactions exclusively (three-body collisions play a role only at pressure values higher than those used in a typical pump-probe spectroscopy experiment). Since the density values for the atomic species interacting with the e.m. field are normally quite low, the only collisions that are important are those between an *active* atom (i.e., interacting with the field) and one of the buffer gas. For most optical experiments, buffer gas species that do not affect the population of the upper state (e.g., alkali atoms in a noble gas atmosphere) are the preferred choice, since they only affect the line broadening and may allow one to perform an experiment with predominant homogenous, rather than inhomogeneous, broadening.

The literature on the consequences of collisions on optical transitions is rather extensive and dates very far back (e.g., Refs. [2,66]). Numerous effects have been discovered, among which are collision-assisted amplification processes [67], modified atomic velocity profiles resulting from the in-

terplay between collisions and Doppler broadening [63], changes in the optical lines in saturation spectroscopy [68], and thermalization processes leading to gain enhancement [54,55].

The problem that we analyze centers on the off-resonance interaction of a (strong) pump and a (weak) probe beam with a thermal sample of two-level atoms placed in a thermal bath—hence, with collisions. We consider a collinear, counterpropagating geometry for pump and probe and study the interaction including: atomic motion, momentum transfer, and collisions. The interaction, as in Refs. [53–55] is evaluated at the position of the individual atom, which possesses a determined velocity. This choice differs from the common one, which considers the interaction to be nonlocal (even in the more general treatments, e.g., Ref. [38]). Collisions are introduced in a standard way used in molecular dynamics (see, e.g., Ref. [69]) and the time evolution of each individual atom is evaluated. The approach is similar to that followed in many problems in statistical physics, and already introduced in optics in Ref. [70]. The results that we present are a mostly analytical extension of the general treatment of pump-probe spectroscopy which include atomic motion, momentum transfer, collisions, and the contribution of the scattered field to the global field, thereby providing a feedback mechanism which couples the behavior of e.m. field and atoms.

As such, this paper represents an additional step in the description of pump-probe spectroscopy with counterpropagating beams, which finds its most extensive and careful treatment in Ref. [25]. There, the absorption spectrum of a weak beam, as a function of detuning, was studied, including propagation effects and Doppler broadening (in variable amount); a very detailed interpretation of the physical mechanisms that lead to gain was offered (nonlinear phasing by an external field applied to the oscillators, whose eigenstates and eigenfunctions are renormalized by the same strong pump field). In that work [25], the atomic recoil was not taken into account, since the description was limited to the semiclassical approximation. Hence, the shape of the velocity distribution was assumed to be fixed, thereby excluding both reshaping (coming from the interaction between individual atoms and field) and overall shifts (due to global radiation pressure). The absence of collisions, in that treatment, prevented the authors from investigating the physics which results from the transfer of atoms from one velocity class to another. Finally, plane waves were assumed for the e.m. field, thereby excluding the possibility of studying effects related to the existence of an external time scale, such as the crossing time for atoms which traverse the interaction volume.

In this paper, we take up the task of fulfilling some of those goals within a semiclassical approach, extended by the recent introduction of a modeling technique, which allows for a correct description of position and momentum of the individual atom [53], and by the introduction of the interaction with an external thermal bath [54,55]. This way, we can self-consistently account for atomic motion and modifications to the velocity classes, for mixing among them (through the action of radiation pressure or dipole forces, but

also through collisions), and also for the presence of external time scales (determined by the collision rate with the atoms of the thermal bath). In spite of a microscopic approach to the description, through suitable approximations we arrive at a state equation for the probe field's amplitude, which predicts the appearance of a phase transition—a result that could not be obtained in the traditional spectroscopic approach.

Section II is devoted to the introduction of the model and to a discussion of the corresponding physical setup. An approximation is introduced here, which reduces the problem to a simpler, but still very meaningful form, where analytical expressions can be obtained for some of the physical variables. In Sec. III, we develop a perturbative approach that allows for the identification of an analytical expression for the transition point. A more general modal expansion is presented in Sec. IV: from it we derive a dynamical equation for the probe field valid also in the nonperturbative regime; its solution requires a numerical support, though. A comparison between the reduced model and the original full model is performed in Sec. V, where several aspects of the numerical simulations are presented as well. Section VI is devoted to a brief summary of our main results and to an outline of the most relevant problems still deserving clarification.

II. THE MODEL

A model describing the interaction between an ensemble of two-level atoms and two counterpropagating e.m. fields, including atomic position and velocity, and momentum transfer due to the photon-atom interaction, was introduced a few years ago [53]. Its mathematical form consists of $5N$ equations describing the single-atom degrees of freedom (real and imaginary part of the polarization S_j , the population difference D_j , the atomic position θ_j , and momentum P_j , normalized to the wavelength and the photon's momentum, respectively, plus two equations for the complex amplitude A_1 of the probe field [71]). In this model, under the approximation of a weak probe, the pump intensity is considered to be constant and is thus treated as a parameter. More precisely, the equations are [53]

$$\dot{\theta}_j = P_j, \quad (1a)$$

$$\dot{P}_j = 2\text{Re}[(A_2 - A_1 e^{i\theta_j})S_j^*], \quad (1b)$$

$$\dot{S}_j = \frac{i}{2}(P_j + 2\Delta_{20})S_j - \rho D_j(A_1 e^{i\theta_j} + A_2) - \Gamma S_j, \quad (1c)$$

$$\dot{D}_j = 4\rho\text{Re}[(A_1 e^{i\theta_j} + A_2)S_j^*] - \Gamma(D_j - D_{eq}), \quad (1d)$$

$$\dot{A}_1 = i\Delta_{21}A_1 + \frac{1}{N} \sum_{j=1}^N S_j e^{-i\theta_j}, \quad (1e)$$

where time is rescaled to $\rho\omega_r$, $\Gamma = \gamma/\rho\omega_r$ is the scaled atomic decay rate (for the sake of simplicity, population inversion and polarization are assumed to decay with the same rate, γ), $\Delta_{20} = (\omega_2 - \omega_0)/(\rho\omega_r)$ and $\Delta_{21} = (\omega_2 - \omega_1)/(\rho\omega_r)$ are the scaled detunings of the input field frequency relative

to the atomic, ω_0 , and probe field, ω_1 , frequencies, respectively, and D_{eq} is the equilibrium population difference ($D_{eq}=1$ in all our simulations). The parameter ρ is defined as $\rho = [(n\wp^2\omega_0)/(2\hbar\epsilon_0\omega_r^2)]^{1/3}$ where \wp is the dipole moment, $\omega_r = 2\hbar k^2/m$ is the recoil frequency, and n is the density of atoms. \hbar is Planck's constant, k is the wave vector of the e.m. field (since the pump and probe frequencies are very close to each other, the modulus of the two wave vectors is assumed to be the same), m is the atomic mass, and ϵ_0 is the dielectric constant of vacuum. The atomic momentum has been rescaled to the photon's momentum, $P_j = p_j/(\rho\hbar k)$ while the position is normalized to (half) the optical wavelength, $\theta_j = 2kz_j$. A typical set of parameters for a sodium sample with density $n = 10^{19} \text{ m}^{-3}$ is $\omega_r \approx 2\pi \times 10^5 \text{ rad s}^{-1}$, $\rho \approx 1.5 \times 10^3$, $\Gamma = 20 \times \pi \times 10^6/(\rho\omega_r) \approx 0.15$; these parameters are evaluated assuming a temperature $T \approx 550 \text{ K}$. For comparison with previous work [54,55], where the parameters were chosen for ease of numerical integration, in the rest of this work we will use $\rho = 10$, $\Gamma = 1$, $\Delta_{20} = -15$, and $\Delta_{21} = 1$.

Subsequent to its introduction [53], it was noted that this model is not sufficient to describe some experiments, in particular, those performed in hot vapors [58,59]; hence, an extension was proposed in Ref. [54]. There, collisions (with a buffer gas) were included to reproduce actual experimental situations [58,59]. As a result, the atomic motion thermalizes due to the interaction with the reservoir. This extension brings the additional advantage of providing a relaxation mechanism for the atoms, which allows for the appearance of stable, long-term solutions, absent in the original model [53]. In fact, in the original model unphysical effects, such as the permanent presence of an acceleration due to the pump recoil—whose consequence is to push the atoms away from resonance—are removed by introducing a relaxation mechanism for the momentum, in order to simulate the action of actual mechanisms occurring in a real system (e.g., atoms exiting the interaction volume after a certain time, while “fresh” ones enter it). Nonetheless, this is not sufficient to give rise to true steady-state solutions, and strong temporal oscillations characterize the CARL model.

The aim of this paper is to obtain an analytical description of the pump-probe interaction in the nonlinear medium when atomic position, motion, and recoil are taken into account. As it is extremely difficult to find a closed solution to the full CARL model [53], and even more so when collisions are introduced [54,55], a certain number of reasonable approximations need to be made in order to obtain a more tractable (reduced) model. We will check, *a posteriori*, whether they are reasonable by comparing the numerical solutions of the full model (FM) and to those of the reduced model (RM), for which we can write analytical solutions.

Collisions play an important role in many of the pump-probe spectroscopy experiments that can be conducted in an atomic vapor or in a gas. Only in the case of cold atomic samples, which are devoid of a buffer gas and where the medium is sufficiently dilute to entirely neglect the interactions between atoms, is the collisionless approximation valid. This is the case that is best described by the original CARL model [53] if the experiment is run for a limited duration.

The opposite limit, strongly collisional regime, is the one often used when a predominant homogeneous line broadening is desired. In this case, collisions occur so often that the exchange of momentum between e.m. field and atoms plays a negligible role, since the changes in atomic velocity during a collision (e.g., with a buffer gas atom) are orders of magnitude larger than those which occur during the interaction with a photon. This regime is fully and properly described by a homogeneous, collision-dominated, atomic susceptibility and stationary atoms (with, at most, diffusion playing some role in describing their motion).

The situation which we are interested in describing is an intermediate one, where collisions are present (e.g., to keep the atoms from reaching the cell windows where they may chemically react—the case of alkali atoms), but where the dominant broadening is of Doppler origin. This amounts to having in a cell a sufficiently dilute buffer gas [58,59]. Under these conditions, the mechanical effects of light on the atoms are strongest: the atoms are subject to a strong acceleration through nonresonant scattering processes and, also, through radiation pressure. On the other hand, collisions randomly change the velocity of the atoms that interact with the field and can in a single event equilibrate thousands of momentum exchanges with the e.m. field, since the momentum that they exchange is much larger than that of a photon. Hence, the *optimal* situation, as far as the investigation of the *mechanical effects of light* in a spectroscopic problem is concerned, is that where collisions occur seldom enough to let the momentum transfer accumulate, but often enough to allow for sufficient mixing—thus ensuring that an equilibrium condition exists (without renewing the sample). This is exactly the regime that we are interested in investigating in this paper and which can be best handled with our technique.

The specific way collisions are modeled is by generating a random sequence of intercollision times (independently for each atom) distributed according to a Poisson law whose average value will be denoted with t_c . At each collision, the momentum of the colliding, j th, atom is randomly reset according to the Gaussian distribution

$$Q_{eq}(P_j) = \frac{1}{\sqrt{2\pi\sigma}} \exp\left\{-\frac{P_j^2}{2\sigma}\right\},$$

where $\sigma = mk_B T/(\rho\hbar k)^2$ is the rescaled temperature of the buffer gas (k_B is Boltzmann's constant); moreover, the phase of the atomic polarization S_j is also reset to a value uniformly distributed in the whole range $[0, 2\pi]$ [72].

Two approximations are at the heart of the analytical treatment that we propose in this paper. The first one is related to the strength of the probe beam, while the second one is based on the frequency of collisions.

The interaction between one field of arbitrary strength and an ensemble of atoms can be treated exactly (cf., e.g., Ref. [73]). Instead, the addition of the probe field complicates the picture to the point that only a power expansion, which considers the probe intensity as being small, yields manageable results [24,25]. In the following, we adapt this idea and, while we are able to handle analytically the dynamics of the Bloch vectors for arbitrary values of the probe field ampli-

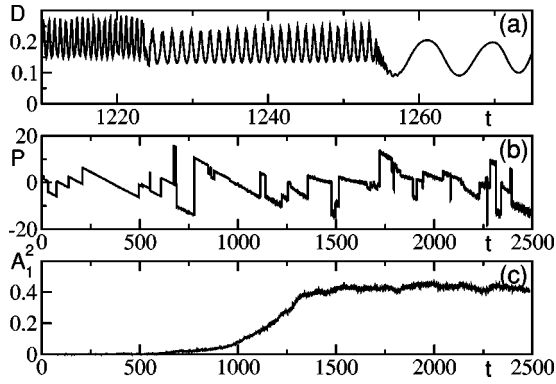


FIG. 1. Time dependence of the population inversion D (a) and of the momentum P (b) of one of 512 atoms in a simulation performed with $\sigma=33$. In panel (c) the probe intensity A_1^2 is plotted.

tude, we consider that the probe field's contribution to the atomic recoil is sufficiently small to be negligible (at least in a first approximation). What we are neglecting is only the amount of momentum transmitted to the atoms in the form of recoil when a probe photon is scattered into the pump beam. This amounts to saying that we consider only the recoil suffered by atoms subjected to the pump field while we neglect the contributions coming from those probe photons that are scattered into the pump field (thereby transferring an opposite amount of momentum onto the atoms). The larger is the imbalance in favor of the pump strength, the better our approximation; this will become clearer at a later stage in the paper. Luckily, there is a further element in our model which extends the validity of the approximation: the occasional collisions mix the atomic velocity distribution, thereby resetting the atomic momentum to a new value and strongly reducing the artificial bias that we introduce in the atomic acceleration by neglecting the mechanical action of the probe field.

The second approximation rests on the frequency with which collisions occur. Numerical integrations of the FM [54,55] indicate the presence of three distinct time scales: a fast one, over which the atomic variables (or Bloch vector) evolve, an intermediate one, controlled by collisions (entirely separate from the atomic one, in the regime that interests us), and a slow one, which describes the time constant with which the probe field evolves. Such a difference of time scales can be appreciated in Fig. 1 where we have plotted a sample of the dynamics of the population inversion and of the momentum of a selected atom [see panels (a) and (b), respectively], and that of the probe field intensity A_1^2 [panel (c)]. From the evolution of the population inversion, D , one can recognize the presence of the various fast rotations arising in dependence of the detuning. Oscillations appear at different frequencies (three different values, in the figure), which are due to the apparent (i.e., Doppler-shifted) detuning between atomic resonance and field frequency. We see that even choosing a short time between collisions [compare the horizontal scale to the panel (b) of the figure], the number of oscillations is large. In addition, panel (a) shows how the transient, necessary to the dipole to reach equilibrium with the external field after the collision, is even much shorter than the time between collisions. Between $t \approx 1254$ and t

≈ 1257 time units very fast oscillations appear, which indicate the dipole's transient evolution between the condition in which it is found after the collision and its relaxation to equilibrium with the driving field. The intermediate time scale is better seen in panel (b), where the momentum dynamics clearly reveals the random resetting due to the collisions. Here, one also recognizes the effect of radiation pressure, which accelerates the atoms towards increasingly negative velocity values (the pump field is oriented opposite to the reference axis). Finally, the longest time scale can be appreciated in panel (c), by looking at the probe intensity.

The fact that collisions are infrequent over the time scale Γ^{-1} characterizing the atomic response, implies that except for a transient following the collision, the *free* evolution of the Bloch vector represents quite accurately the dynamics of the atomic variables. Since, in addition, the field evolves over time scales that are quite long compared to the atomic dynamics and to the typical thermalization time of the momentum which is proportional to t_c , we find ourselves in the fortunate situation where we can consider the field (temporarily) constant. This allows us to handle the problem in a sort of Born-Oppenheimer approximation, where we describe the atomic dynamics as being subject to a constant field between collisions, where the atomic velocity distribution is maintained close to equilibrium by the collisions themselves, and where we can integrate the atomic response over the *short* time scales. This procedure allows us to evaluate the field in closed form, and to feed the result back into the atomic dynamics, thereby closing the loop analytically.

This three-time-scale approach allows us to describe the dynamics of the probe field, which is instead considered to be a parameter in the traditional spectroscopic approach [24,25], and to predict interesting features of the field such as the occurrence of a phase transition, and to analyze its nature.

According to the above arguments, the probability distribution $Q(P)$ of atomic momenta is assumed to be the stationary solution of a kind of Fokker-Planck equation without diffusion and with an added exponential relaxation (as in Ref. [54]):

$$\frac{\partial Q}{\partial t} = -\frac{Q - Q_{eq}}{t_c} - \frac{\partial}{\partial P}(FQ), \quad (2)$$

where the force field $F(P)$ is the radiation pressure

$$F(P) \equiv \dot{P} = -\frac{2D_{eq}\rho A_2^2 \Gamma}{\Gamma^2 + (P/2 + \Delta_{20})^2 + 4\rho^2 A_2^2}, \quad (3)$$

obtained by inserting in Eq. (1b) the stationary solution of the Bloch equation under the approximation of a negligibly small probe field, i.e.,

$$\text{Re}\{S_j\} = -\frac{D_{eq}\rho A_2 \Gamma}{\Gamma^2 + (P_j/2 + \Delta_{20})^2 + 4\rho^2 A_2^2}. \quad (4)$$

For practical reasons, instead of solving the Fokker-Planck equation, Eq. (2), we prefer generating momenta according to the Gaussian distribution Q_{eq} and modifying P as if each

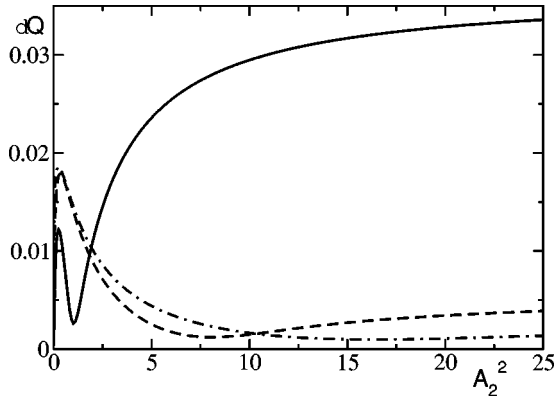


FIG. 2. δQ as a function of the pump field intensity A_2^2 for different temperatures $\sigma=33$ (solid), $\sigma=233$ (dashed), and $\sigma=433$ (dot-dashed).

atom were exposed to a constant radiation pressure [i.e., we assume a constant P in the rhs of Eq. (3) for a fixed time t_c]. From Fig. 2 one can verify that the resulting numerical error is always negligible in the various regimes we have considered in this paper. There, we have indeed plotted the integrated error

$$\delta Q = \int dP |Q(P) - \tilde{Q}(P)|,$$

where $\tilde{Q}(P)$ is the distribution resulting from the above described procedure, versus the pump intensity for three different temperature values. The error is always negligible.

From this analysis of the momentum distribution we conclude that the approximation of a shifted Gaussian velocity shape, due to radiation pressure, represents an acceptable approximation as long as small values of ρ are considered (i.e., very low atomic densities), and that the interaction with only one field is considered. The addition of a probe, even in the low-density case, significantly perturbs the velocity distribution to a point that the dynamics of the external atomic degrees of freedom must be taken into account.

III. PERTURBATIVE EXPANSION

The goal of this and of the following section is to eliminate the atomic variables under the approximation that P_j evolves on a time scale longer than this latter variable and thus can be treated as a constant. Before entering into the technical details, let us notice that the correctness of such an approach depends crucially on the assumption that t_c is long enough to ensure the convergence of the Bloch dynamics towards the asymptotic solution. It is obvious that no matter how long t_c is, there is always a fraction of atoms $\approx \Gamma/t_c$ for which this is not true. Our approach will hold for all those cases where the number of atoms whose internal variables are in a transient state is small. This does not represent a very strong restriction, since interesting effects are observed even when the collisions are sufficiently rare. In the numerical simulations performed in Ref. [54], for instance, the fraction of atoms for which our approximation breaks down is very small ($\approx 2\%$).

According to the discussion of the preceding section, we assume P_j to be constant and thus consider it as a parameter rather than a variable. Hence, the normalized atomic position θ becomes a linear variable of time and we redefine it as $\theta_j = \theta_j^0 + P_j t$. This approximation is the starting point for understanding and describing the numerically observed phase transition. Within this framework, we have the following set of $3N+2$ equations:

$$\begin{aligned} \dot{S}_j &= (-\Gamma + ip_j)S_j - \mu D_j [1 + E e^{i(P_j t + \theta_j^0 + \psi)}], \\ \dot{D}_j &= -\Gamma(D_j - D_{eq}) + 4 \mu \text{Re}\{[1 + E e^{i(P_j t + \theta_j^0 + \psi)}]S_j^*\}, \end{aligned}$$

$$\dot{E} = \frac{1}{A_2} \text{Re}\{C\},$$

$$\dot{\psi} = \Delta_{21} + \frac{1}{A_2 E} \text{Im}\{C\}, \quad (5)$$

where

$$C = \frac{1}{N} \sum_{j=1}^N S_j \exp[-i(P_j t + \theta_j^0 + \psi)]. \quad (6)$$

The detuning Δ_{20} has been absorbed into the definition of the new parameters $p_j = P_j/2 + \Delta_{20}$ and we have introduced the rescaled amplitude E and the phase ψ of the probe field A_1 ($A_1 = A_2 E e^{i\psi}$). Another useful parameter, which coincides with the control parameter of the phase transition, is the normalized Rabi frequency $\mu = \rho A_2$ [53] (hence, in physical units, the Rabi frequency is $\Omega_r = \rho^2 A_2 \omega_r$).

In the thermodynamic limit ($N \rightarrow \infty$), the sum in the definition of C transforms into an integral over the distribution of the instantaneous phases θ_j^0 . In the approximation of a small recoil effect, the integral writes as a double integral over the distribution $Q(P)$ of momenta and over the (flat) distribution of initial angles θ^0 (there is no longer the need to use the subscript j as θ_0 and P are now free parameters that define a specific class of atoms—i.e., we are considering the limit of the continuum):

$$C = \frac{1}{2\pi} \int_{-\infty}^{+\infty} \int_0^{2\pi} S \exp[-i(Pt + \theta^0 + \psi)] Q(P) dP d\theta_0. \quad (7)$$

Numerical simulations suggest that in the stationary regime the field's amplitude E is constant while its phase ψ increases linearly in time. Indeed, it is easy to verify that this is a formally acceptable solution of the above set of equations. *A fortiori*, in the vicinity of the phase transition, we can, in a first approximation, neglect the dynamics of E (critical slowing down) and assume that

$$\psi(t) = \Delta t, \quad (8)$$

for some Δ value to be determined self-consistently (without loss of generality, we have chosen the time origin in such a way that the field phase is 0).

After introducing a shifted time variable,

$$\tau = t + \frac{\theta^0}{\omega}, \quad (9)$$

where $\omega = P + \Delta$ is the Doppler-shifted frequency (in the rotating reference frame) of the field seen by the atoms of the velocity class that we are considering, the atomic equations become

$$\begin{aligned} \dot{S} &= -aS - \mu D(1 + Ee^{i\omega\tau}), \\ \dot{D} &= -\Gamma(D - D_{eq}) + 4\mu \text{Re}[(1 + Ee^{i\omega\tau})S^*], \end{aligned} \quad (10)$$

where we have also introduced the complex variable $a = \Gamma - ip$.

These are the equations of a parametrically forced linear oscillator. In view of the smallness of E , one can formally expand S and D as follows (cf., e.g., Ref. [25] where the case $\Delta = 0$ is treated):

$$\begin{aligned} S(\tau) &= \sum_{m=0}^{\infty} s_{[m]} E^m, \\ D(\tau) &= \sum_{m=0}^{\infty} d_{[m]} E^m. \end{aligned} \quad (11)$$

By inserting Eqs. (11) into Eqs. (10), one obtains

$$\begin{aligned} \dot{s}_{[0]} &= -as_{[0]} - \mu d_{[0]}, \\ \dot{d}_{[0]} &= -\Gamma(d_{[0]} - D_{eq}) + 2\mu(s_{[0]} + s_{[0]}^*), \end{aligned} \quad (12)$$

and the recursion relation for all other orders:

$$\begin{aligned} \dot{s}_{[m]} &= -as_{[m]} - \mu(d_{[m]} + d_{[m-1]}e^{i\omega\tau}), \\ \dot{d}_{[m]} &= -\Gamma d_{[m]} + 2\mu(s_{[m]} + s_{[m]}^*) + 2\mu[s_{[m-1]}e^{-i\omega\tau} \\ &\quad + s_{[m-1]}^*e^{i\omega\tau}]. \end{aligned} \quad (13)$$

For $m > 0$, Eqs. (12) admit the stationary solution [cf. also Eq. (4)]

$$s_{[0]} = -\frac{\mu}{a} d_{[0]}, \quad (14)$$

$$d_{[0]} = \frac{D_{eq}|a|^2}{|a|^2 + 4\mu^2}, \quad (15)$$

which is the well-known expression for the Bloch model under the action of a single field. From Eqs. (13), one can see that the expression for the m th order contains terms rotating at the frequency $\pm \omega$ multiplied by the $(m-1)$ th contributions. Accordingly, one can write

$$\begin{aligned} s_{[m]} &= \sum_{n=0}^m s_{(2n-m)}^{[m]} e^{i(2n-m)\omega\tau}, \\ d_{[m]} &= \sum_{n=0}^m d_{(2n-m)}^{[m]} e^{i(2n-m)\omega\tau}. \end{aligned} \quad (16)$$

By inserting the preceding Fourier expansions in Eqs. (7), and exploiting the definitions of τ and ω , one immediately recognizes that the only nonzero contributions to the integral arise when the phase factor is strictly zero, which happens only when $2n - m = 1$, since we are assuming that the thermal noise induced by the buffer gas ensures a flat distribution of the θ^0 [74]. This implies that only the odd terms may contribute:

$$C = \sum_{\text{odd } m}^{\infty} E^m c_{[m]}, \quad (17)$$

where

$$c_{[m]} = \int_{-\infty}^{+\infty} s_{(1)}^{[m]}(P) Q(P) dP, \quad (18)$$

since the integral over the initial phase θ_0 factors out. The expressions for field amplitude and phase [cf. Eqs. (5)] then take the form

$$\begin{aligned} \dot{E} &= \frac{1}{A_2} [\text{Re}\{c_{[1]}\}E + \text{Re}\{c_{[3]}\}E^3 + \dots], \\ \dot{\psi} &= \Delta_{21} + \frac{1}{A_2} [\text{Im}\{c_{[1]}\} + \text{Im}\{c_{[3]}\}E^2 + \dots]. \end{aligned} \quad (19)$$

We have analytically determined both the first and the third order term: the derivation of $c_{[1]}$ is reported in Appendix A, while the expression for $c_{[3]}$ has been obtained with MAPLETM. Since its derivation is analogous to that of $c_{[1]}$ and given that the final expression is extremely long, we do not give its explicit form. The change in sign, from negative to positive, of $\text{Re}\{c_{[1]}\}$ signals the onset of the change from a zero to a finite value for the field E through a Hopf bifurcation. The frequency of the bifurcating solution is determined from $\text{Im}\{c_{[1]}\}/A_2$, as shown by the phase equation; this frequency corresponds to a value of $\Delta = \Delta_{21} + \text{Im}\{c_{[1]}\}/A_2$. Finally, the sign of the real part of the cubic term determines the character of the bifurcation (supercritical or subcritical). We shall see in Sec. V that both scenarios can arise.

IV. MODAL EXPANSION

In the preceding section, we have seen how the atomic degrees of freedom can be perturbatively eliminated when the field amplitude is small, but the results which we have obtained hold only in a small neighborhood of the transition point. Here, we follow a different approach, which allows us to describe the problem even far from the phase transition. By assuming that the field amplitude is a slow variable

(which is certainly true in the vicinity of any stationary solution, whether stable or not), the dynamics of the atomic variables is described by the parametrically forced oscillator equations, Eqs. (10), described in Sec. III. Accordingly, we expect the dynamics to converge towards a periodic solution with period $T = 2\pi/\omega$, but such a solution can possess many Fourier harmonic components. An effective method for determining the asymptotic solution consists in expanding the variables in Fourier modes with fundamental frequency ω ,

$$S(t) = \sum_{n=-\infty}^{+\infty} S_{(n)} e^{in\omega t},$$

$$D(t) = \sum_{n=-\infty}^{+\infty} D_{(n)} e^{in\omega t}, \quad (20)$$

where we denote $D_{(n)}^* = D_{(-n)}$, $D(t)$ being a real variable. By inserting Eqs. (20) into Eqs. (10), one obtains

$$S_{(n)} = -\mu f_{(n)} [D_{(n)} + ED_{(n-1)}], \quad (21)$$

$$(\Gamma + in\omega)D_{(n)} = \Gamma D_{eq} \delta_{n0} + 2\mu [S_{(n)} + S_{(-n)}^* + E(S_{(n+1)} + S_{(-n+1)}^*)], \quad (22)$$

where we have introduced

$$f_{(n)} = \frac{1}{a + in\omega}. \quad (23)$$

Using the property $D_{(-n)}^* = D_{(n)}$, it is readily clear that

$$S_{(-n)}^* = -\mu f_{(-n)}^* [D_{(n)} + ED_{(n+1)}]. \quad (24)$$

Inserting Eqs. (21) and (24) into Eq. (22), we obtain

$$\begin{aligned} & -(\Gamma + in\omega)D_{(n)} + \Gamma D_{eq} \delta_{n0} \\ & = 2\mu^2 \{ [f_{(n)} + f_{(-n)}^* + E^2(f_{(n+1)} + f_{(1-n)}^*)] D_{(n)} \\ & \quad + E[f_{(n)} + f_{(1-n)}^*] D_{(n-1)} \\ & \quad + E[f_{(n+1)} + f_{(-n)}^*] D_{(n+1)} \}, \end{aligned} \quad (25)$$

which can be written in the more compact form

$$\eta_{(n)} D_{(n)} + \beta_{(n-1)} D_{(n-1)} + \beta_{(n)} D_{(n+1)} - \frac{\Gamma D_{eq}}{2\mu^2} \delta_{n0} = 0, \quad (26)$$

where

$$\eta_{(n)} = \frac{\Gamma + in\omega}{2\mu^2} + f_{(n)} + f_{(-n)}^* + E^2 \{ f_{(n+1)} + f_{(1-n)}^* \}, \quad (27)$$

$$\beta_{(n)} = E \{ f_{(-n)}^* + f_{(n+1)} \}. \quad (28)$$

The infinite set of linear equations, Eq. (26), can be solved by introducing the variable

$$W_{(n)} = \frac{\beta_{(n)} D_{(n+1)}}{\eta_{(n)} D_{(n)}}. \quad (29)$$

In fact, substitution of Eq. (29) into Eq. (26) yields, for $n \neq 0$, the following recursion relation

$$W_{(n-1)} = -\frac{\alpha_{(n)}}{1 + W_{(n)}}, \quad (30)$$

where

$$\alpha_{(n)} = \frac{\beta_{(n-1)}^2}{\eta_{(n)} \eta_{(n-1)}}. \quad (31)$$

For $n=0$, observing that $\beta_{(-1)} = \beta_{(0)}^*$, one finds

$$D_{(0)} = \frac{\Gamma D_{eq}}{2\mu^2 \eta_{(0)}} \frac{1}{1 + W_{(0)} + W_{(0)}^*}. \quad (32)$$

Finally, the source term for the field equation, $S_{(1)}$, can be expressed as

$$\begin{aligned} S_{(1)} & = -\mu f_{(1)} [D_{(1)} + ED_{(0)}] \\ & = -\frac{\Gamma D_{eq} f_{(1)}}{2\mu \eta_{(0)} \beta_{(0)}} \frac{\eta_{(0)} W_{(0)} + \beta_{(0)} E}{1 + W_{(0)} + W_{(0)}^*}. \end{aligned} \quad (33)$$

The explicit expression for the polarization requires only the knowledge of $W_{(0)}$, which in turn needs the numerical values for η_0 , η_1 , α_1 , and β_0 . The latter quantities are all defined in terms of the momentum value and the other parameters, and are therefore known. $W_{(0)}$ is obtained iterating back from the higher-order components. Since the values for W_n tend rapidly to zero for increasing values of n , it suffices to choose a value of $n=m$ sufficiently large and a small value of W_m (e.g., $W_m=0$) as an initial condition. The calculations are very quick and one rapidly obtains convergence towards a trajectory, independently of the choices made for m and the value of W_m .

By integrating the contributions arising from all different velocities, each weighted according to the proper distribution, we obtain the equations for the probe field amplitude and phase:

$$\dot{E} = \frac{1}{A_2} \text{Re}\{C(E, \psi, \mu, \sigma)\} := -\frac{dU}{dE}, \quad (34)$$

$$\dot{\psi} = \Delta_{21} + \frac{1}{EA_2} \text{Im}\{C(E, \psi, \mu, \sigma)\}, \quad (35)$$

where $U(E)$, implicitly defined by the last equality in Eq. (34), plays the role of a potential controlling the field dynamics.

V. NUMERICAL RESULTS

The overall response of the whole ensemble of atoms can be obtained by summing the contributions of each velocity class. In Fig. 3 we have reported the linear response $s_{(1)}^{[1]}$ to

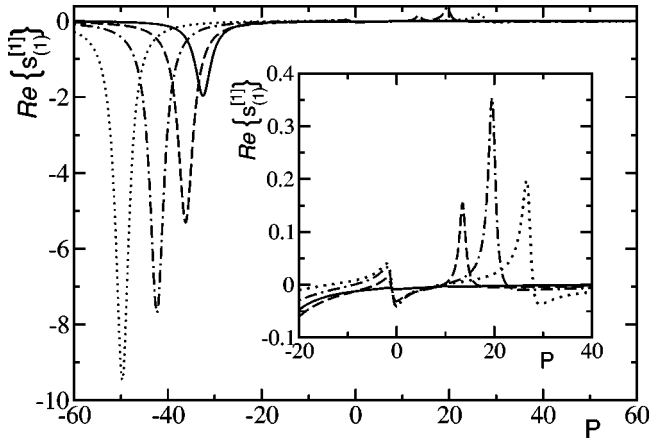


FIG. 3. Value of $s_{(1)}^{(1)}$ for each class of velocity P for different amplitudes of the pump field A_2 : 0.2 (solid), 0.6 (dashed), 1 (dotted-dashed), 1.4 (dotted).

an infinitesimal field E for different values of μ . The zero field ($E=0$) state is unstable and thus can grow to a finite value only if the average value of $s_{(1)}^{(1)}$ is positive. The average has to be performed over the distribution of velocities that is basically a slightly shifted Gaussian.

The largest response corresponds to the negative peak, located on the negative side of the momentum distribution (we recall that the pump field is oriented against the reference axis). These peaks correspond to absorption of the probe field, since the quantity plotted is the value of the growth rate of the field itself [cf. first equation in Eqs. (19)].

We see how, for increasing pump power A_2^2 , the absorption grows in value and moves to decreasing values of momentum, as is to be expected. The inset shows the characteristic presence of the Rayleigh scattering feature (placed at momentum values near zero), followed, to the right, by the positive (amplification) peak originating from the usual three photon gain. At fixed temperature (i.e., fixed width of the velocity spread), upon increasing the Rabi frequency, μ , it is possible to encounter the situation where the absorption peak (left) is located in the tails of the momentum distribution, while the gain feature is placed in a region well populated by the moving atoms. The weighted integration over the (finite) Doppler distribution gives a measure of the global response for the probe. In the situation just described, the effect of the absorption peaks is negligible, while the three photon gain dominates in the frequency interval corresponding to the detuning values induced by the atomic motion. Hence, an overall gain ensues (i.e., an instability of the $E=0$ solution). This situation has already been carefully described in Ref. [25], and the detailed physical interpretation offered there holds for our current results, even though we are including recoil (due to the pump field), and therefore also the shift and (partial) deformation of the momentum distribution itself.

The integration over the velocity profile provides analytical predictions for the steady-state value of the probe field which results from the interaction with the pumped medium. To test their validity, these predictions should be compared to the numerical integration of the set of equations that describe the model. In Fig. 4 we perform this check by showing the

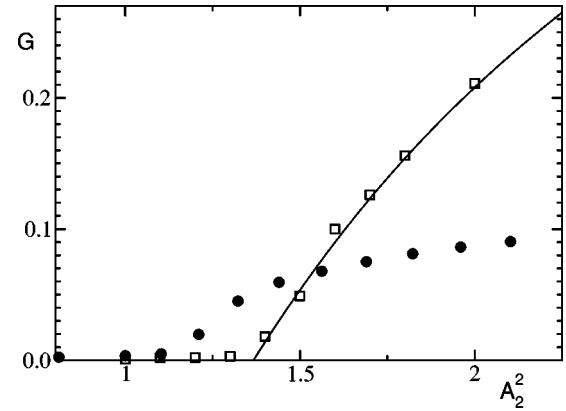


FIG. 4. The gain $G=A_1^2/A_2^2$ vs the pump intensity A_2^2 . Full circles correspond to the numerical data for the original model, squares correspond to the reduced model, while the solid curve is the output of after the modal expansion described in the preceding section.

analytical results (solid line) and the numerical ones obtained from the FM (solid circles) or the RM (open squares).

Figure 4 clearly shows that the analytical calculations based on the Fourier expansion (Sec. IV) provide an excellent agreement with the numerical results coming from the RM (compare solid line with open squares). The quality of this agreement, coupled to the fact that convergence is achieved in a few iterations, renders the approach an extremely powerful and successful one for describing the onset of the phase transition and to follow the functional dependence of the probe field amplitude on the pump amplitude even in the regime where it is not small.

On the other hand, in the figure we notice a discrepancy between the numerical results obtained from the FM and the RM. The shift in the bifurcation point, which amounts to about 20% of its absolute value, shows that the action of the probe onto the atomic momentum distribution is not entirely negligible (cf. Sec. VI for further comments). The feedback that the (extremely weak) probe introduces in the atomic sample appears to be sufficient to anticipate the transition, probably by increasing the coherence among the atomic polarization phases. This same contribution is also responsible for an earlier saturation.

An important question to address is the dependence of this scenario on temperature. In the simulations performed in Ref. [54], the value $\sigma=33$ (corresponding to a few mK) was considered since larger values would have required too small an integration time step to be affordable. Since our partially analytical approach can be efficiently used at higher temperatures, we have investigated the bifurcation diagram for larger values of σ . The results are reported in Fig. 5, where one remarks that the onset of a backward field, above a certain temperature, grows out of a first-order phase transition, i.e., it is accompanied by a hysteretic region. A pictorial representation, providing a better understanding of the dynamics of the probe field amplitude E , is given by the effective potential $U(E)$. In Fig. 6, we indeed see that, upon increasing the pump intensity, the system passes from a regime where the $E=0$ field state is stable (cf. the solid curve), to an in-

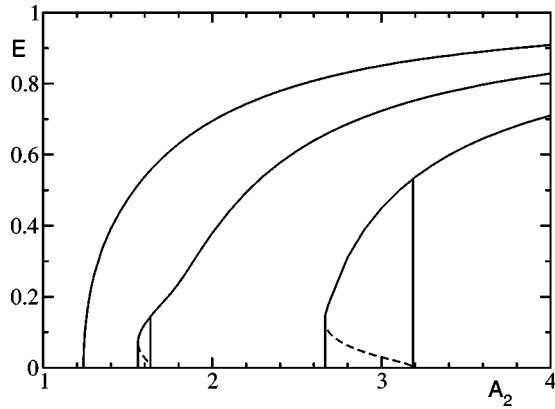


FIG. 5. The bifurcation diagram for different temperature values: from left to right the curves refer, respectively, to $\sigma=33$, 200, and 500.

intermediate one characterized by two minima (dashed line) and, eventually, to a single nonzero minimum (dotted line).

The bistable behavior is the result of a complicated mechanism, within the atomic sample, which gives rise to probe gain. In Fig. 7, we show an example of this complex behavior without attempting a detailed interpretation of the observations. In this figure, one remarks that several peaks and dips develop upon increasing probe field strength E . The dip displayed by the solid curve (which corresponds to $E=0.06$) around $P=-33$ is responsible for stabilizing the overall behavior (for $A_2=2.8$) that would be otherwise unstable for $\sigma=1000$ (dashed line). However, upon further increasing E to 0.32 (dotted-dashed curve), we see that the huge well on the left disappears so that, in spite of many newly born negative dips, the response destabilizes again. It is clear that a general theory would require a description of many different details.

A compact way of summarizing the dependence on the temperature can be obtained by plotting the lower and upper bounds of the hysteretic region where the zero-field and finite amplitude solutions coexist. The upper curve reported in Fig. 8 always corresponds to the stability threshold of the

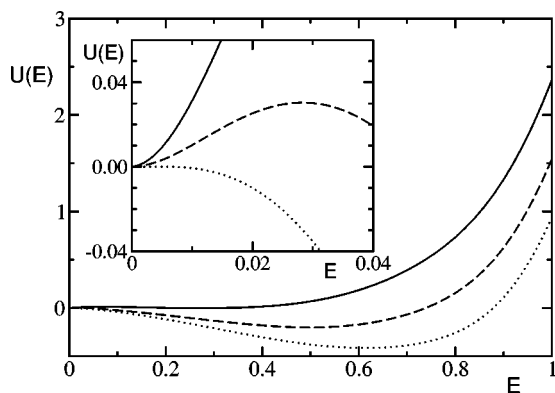


FIG. 6. The effective potential for three different values of μ (40, 43, 47, corresponding to solid, dashed, and dotted curves, respectively) and for $\sigma=1000$. In the inset, an enlargement of the region around $E=0$ is reported to clearly indicate the bistable region.

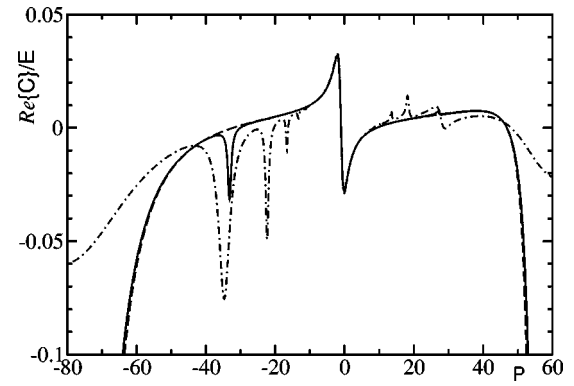


FIG. 7. Response for each class of velocity P for different amplitudes of the probe E (0, 0.06, and 0.32 correspond to dashed, solid, and dotted-dashed lines, respectively) and the same pump amplitude $A_2=2.8$.

zero-field solution, the lower one (for $\sigma_c \geq 140$) is the minimum amplitude guaranteeing the existence of a nonzero field solution. It is interesting to notice that beyond the plateau, which exists at relatively low temperatures, the critical intensity required to generate a coherent field grows linearly with the temperature.

VI. CONCLUSIONS AND PERSPECTIVES

In this paper we have studied a model for the resonant interaction between electromagnetic waves and a gas of atoms in the presence of recoil, showing that to a large extent all the atomic degrees of freedom (internal variables, position, and momentum) can be eliminated. As a result, the model reduces to one complex differential equation for the probe in strong analogy with the equation describing the onset of laser action when atomic polarization and population inversion can be adiabatically eliminated. The present problem, however, is more complicated. The adiabatic elimination of the internal atomic degrees of freedom, as in the more classic laser problem, is made possible by the relatively strong stability of the Bloch equation. Nonetheless, our

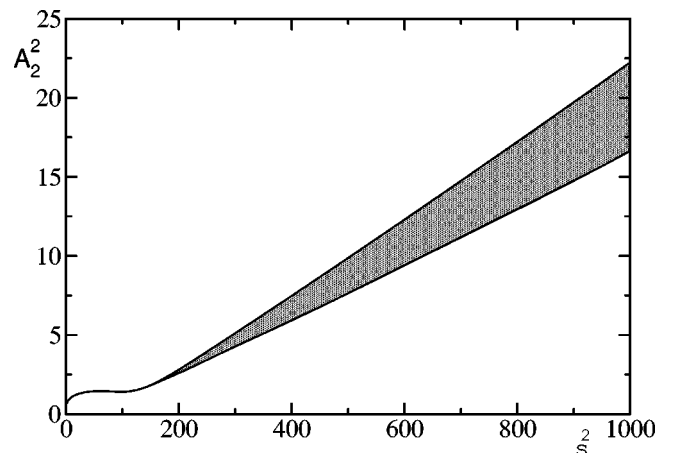


FIG. 8. The lower and upper bounds of the hysteretic region as a function of the temperature σ . The transition becomes first order above the critical temperature $\sigma_c \approx 140$.

elimination technique is more complex than the standard, straightforward one, which even fails to predict the existence of a transition point for this problem. Indeed, once one realizes that the problem amounts to finding the asymptotic solution of a parametrically modulated linear system, it is also clear that an extension of the method already adopted in Ref. [25] is the most effective tool for solving it. The major difficulty arises from the periodic modulation induced by the probe field which, in turn, obliges us to find a sufficiently accurate solution for a wide range of time scales (due to the different detunings induced by the thermal motion).

Less justified is the elimination of position and momentum variables. Indeed, although our approach reproduces the transition point with a reasonable accuracy (20%), the smallness of the deviation is due to the smallness of the probe field amplitude rather than to the accuracy of the description of momentum dynamics. We expect that in regimes where probe and pump fields are comparable, a more detailed model is needed. This is all the more crucial, once we recall that even the starting model was derived under the approximation of a negligibly small probe field. In the meantime, a model has been introduced which does not suffer the same limitation, the so-called cavity model [75]. It will be certainly interesting to extend to that context the approach described in this paper.

From a purely dynamical point of view, in this paper we can only claim to have reduced the number of variables from the initial $5N+2$ to $2N+2$. A complete reduction to two equations (for the amplitude and phase of the field) will only be possible after an accurate analysis of the momentum dynamics. This point is currently under investigation.

A further, more general, comment concerns the structure of the model itself, which is partly mesoscopic and partly microscopic. In fact, the presence of the loss term Γ indicates that spontaneous emission is treated as if the population inversion D_j and the atomic polarization S_j referred to an ensemble of atoms. This is in contrast to the way collisions are introduced, which requires that the label j refers to a single atom. One way out to a more consistent treatment would be the introduction of a fully microscopic model, where spontaneous emission is simulated by a stochastic process occurring at random times (as proposed in Ref. [70] in the absence of recoil). Preliminary studies indicate that one such model reproduces basically the same macroscopic behavior, but the elimination of the microscopic variables cannot be carried out in the same way, since their evolution would be no longer dissipative.

A last remark concerns the observability of the present predictions. In Appendix B we offer an order of magnitude estimate of the transition temperature that marks the onset of the first-order phase transition. We see that for realistic values of the parameters (laser power and beam size) the transition temperature for a sodium atom is situated around the millikelvin. Current technology allows one to realize these conditions quite readily. Our calculations are based on the presence of collisions, which thermalize the sample, and this is not very realistic for an actual experiment. Indeed, most setups which reach such temperatures are (almost) devoid of atomic collisions—due to the low atomic density values that

are typically reached, and to the typical absence of a sufficiently cold buffer gas. However, the short interaction times used for the measurements (due to the limited amount of time for which a trap can be switched off, or to the atomic transit time, for a collimated atomic beam) could remove the need for this ingredient. In fact, in our calculations collisions play the role of a reservoir which ensures the existence of an asymptotic equilibrium, when the atoms are subject to the interaction for a long time. Repeated, averaged measurements performed for short times over different realizations would probably produce results that are similar to those which we predict here. This last point needs, however, specific numerical tests, which we plan to perform in near future.

ACKNOWLEDGMENTS

We wish to thank L. M. Narducci, M. Perrin, and L. Furfaro for very useful discussions. One of us (G.L.L.) is grateful to W. Lange and J. R. Rios Leite for a very fruitful discussion and to W. Lange for a careful reading of the Introduction.

APPENDIX A

The stationary equations for the first-order (in E) terms are of the form

$$s_{(1)}^{[1]} = -\frac{\mu}{a+i\omega}(d_{(1)}^{[1]}+d_{(0)}),$$

$$s_{(1)}^{[-1]} = -\frac{\mu}{a-i\omega}d_{(1)}^{[-1]},$$

$$(\Gamma+i\omega)d_{(1)}^{[1]} = 2\mu[s_{(1)}^{[1]}+(s_{(1)}^{[-1]})^*]+2\mu s_{(0)}^*. \quad (\text{A1})$$

By exploiting the equality $d_{(1)}^{[1]}=(d_{(1)}^{[-1]})^*$, one can write the last of the above equations as

$$\left[\frac{\Gamma+i\omega}{2\mu^2} + \frac{2(\Gamma+i\omega)}{(a+i\omega)(a^*+i\omega)} \right] d_{(1)}^{[1]} = \frac{s_{(0)}^*}{\mu} - \frac{d_{(0)}}{a+i\omega}. \quad (\text{A2})$$

Upon inserting expression (12) for the zeroth-order contributions, one eventually obtains

$$d_{(1)}^{[1]} = -D_{eq} \frac{2a\mu^2}{(|a|^2+4\mu^2)} \times \frac{(2\Gamma+i\omega)(a^*+i\omega)}{(\Gamma+i\omega)[(a+i\omega)(a^*+i\omega)+4\mu^2]}. \quad (\text{A3})$$

Equation (A3) and the first of Eqs. (A1) yield the integrand to be replaced in Eq. (6) in order to obtain $c_{(1)}$,

$$\begin{aligned}
 c_{(1)} = & \int_{-\infty}^{+\infty} \frac{-\mu}{a+i\omega} \frac{D_{eg}|a|^2}{|a|^2+4\mu^2} \\
 & \times \left(1 - \frac{2\mu^2(2\Gamma+i\omega)(a^*+i\omega)}{a^*(\Gamma+i\omega)[(a+i\omega)(a^*+i\omega)+4\mu^2]} \right) \\
 & \times Q(P)dP. \tag{A4}
 \end{aligned}$$

APPENDIX B

An estimate for the growth rate of the upper bound of the bistable region, as a function of temperature, can be obtained using the perturbative expression for $s_{(1)}^{[1]}$, Eq. (A1). From it, one can find the strong absorption peaks that determine the transition from global gain to loss (after integration over the Doppler profile). A straightforward analysis of the expression, Eq. (A1), reveals that the absorption peaks are located at the values of momentum satisfying the second-order polynomial:

$$\begin{aligned}
 & \text{Re}\{(a+i\omega)(a^*+i\omega)+4\mu^2\} \\
 & = \text{Re}\left\{-\frac{3}{4}P^2+(\Delta_{20}-\Delta)P+\Gamma^2+4\mu^2+\Delta_{20}^2-\Delta^2\right\},
 \end{aligned}$$

whose roots are

$$\begin{aligned}
 P_{+,-} = & \frac{2}{3}(\Delta_{20}-\Delta) \\
 & \pm \sqrt{\frac{4}{9}(\Delta_{20}^2-\Delta^2)+\frac{4}{3}(\Gamma^2+4\mu^2+\Delta_{20}^2-\Delta^2)}. \tag{B1}
 \end{aligned}$$

To obtain an order of magnitude for the critical temperature of the upper bound of the bistable region, one can as-

sume that the Doppler width must be narrower than (or at most be as large as) the roots $P_{+,-}$. Indeed, if this is the case, the tails of the momentum distribution are going to strongly reduce the importance of the absorption peaks in the (weighted) integral which measures the atoms' response to the probe. This condition translates into

$$\begin{aligned}
 \pm\sqrt{\sigma} \lesssim & \frac{2}{3}(\Delta_{20}-\Delta) \\
 & \pm \sqrt{\frac{4}{9}(\Delta_{20}^2-\Delta^2)+\frac{4}{3}(\Gamma^2+4\mu^2+\Delta_{20}^2-\Delta^2)}.
 \end{aligned}$$

At large σ values, both detunings and the dissipation can be neglected, so that $\mu^2 \sim \sigma$ as observed in Fig. 8. In such a regime, upon introducing the definitions of μ and σ , one finds the following lower bound for the critical temperature T_c ,

$$k_b T_c \sim \hbar \frac{\Omega_r^2}{\omega_r}, \tag{B2}$$

where k_b is the Boltzmann factor, Ω_r the Rabi frequency of the pump field, and ω_r is the recoil frequency.

In the case of sodium atoms interacting through the D_2 line, $\omega_r \approx 6.23 \times 10^5 \text{ rad s}^{-1}$, while a reasonable estimate of the available laser power (considering a ‘‘top hat’’ distribution [76]) is $P_{las} \approx 1 \text{ mW}$ for a beam of radius $w \approx 4 \text{ mm}$, which corresponds to a Rabi frequency $\Omega_r \approx 10^7 \text{ rad s}^{-1}$. By recalling that $k_B \approx 1.38 \times 10^{-23} \text{ J K}^{-1}$ and $\hbar \approx 1.055 \times 10^{-34} \text{ J s}$, the critical temperature turns out to be

$$T_c \approx 1 \text{ mK},$$

a value experimentally accessible.

-
- [1] I.I. Rabi, Phys. Rev. **51**, 652 (1937).
 [2] J.H. van Vleck and V.F. Weisskopf, Rev. Mod. Phys. **17**, 227 (1945).
 [3] R. Karplus and J. Schwinger, Phys. Rev. **73**, 1020 (1948).
 [4] S.H. Autler and C.H. Townes, Phys. Rev. **100**, 703 (1955).
 [5] M.C. Newstein, Phys. Rev. **167**, 89 (1968).
 [6] R.K. Wangsness and F. Bloch, Phys. Rev. **89**, 728 (1953).
 [7] L. Allen and J.H. Eberly, *Optical Resonance and Two-Level Atoms* (Dover, New York, 1987).
 [8] D. Suter, *The Physics of Laser-Atom Interactions* (Cambridge University Press, Cambridge, 1997).
 [9] Throughout this paper we call feedback the *reaction* of the field structure, coming from the superposition of the counter-propagating pump and probe, on the atomic variables: position and momentum. This *reaction* closes the loop which sees the atoms modify the field configuration (relative amplitude and phase) and the field act back onto the atoms modifying their positions and speeds.
 [10] S.G. Rautian and I.L. Sobel'man, Zh. Éksp. Teor. Fiz. **41**, 456 (1961) [Sov. Phys. JETP **14**, 328 (1962)].
 [11] S.G. Rautian and I.L. Sobel'man, Zh. Éksp. Teor. Fiz. **44**, 934 (1963) [Sov. Phys. JETP **17**, 635 (1963)].
 [12] S.G. Rautian, Proc. Phys. Inst. Acad. Sci. USSR **43**, 1 (1968).
 [13] A. Dienes, Phys. Rev. **174**, 400 (1968).
 [14] A. Dienes, Phys. Rev. **174**, 414 (1968).
 [15] B.R. Mollow, Phys. Rev. **5**, 1522 (1972).
 [16] F. Schuda, C.R. Stroud, Jr., and M. Hercher, J. Phys. B: At. Mol. Phys. **7**, L198 (1974).
 [17] F.Y. Wu, R.E. Grove, and S. Ezekiel, Phys. Rev. Lett. **35**, 1426 (1975).
 [18] R.E. Grove, F.Y. Wu, and S. Ezekiel, Phys. Rev. A **15**, 227 (1977).
 [19] F.Y. Wu, S. Ezekiel, M. Ducloy, and B.R. Mollow, Phys. Rev. Lett. **38**, 1077 (1977).
 [20] B.R. Mollow, Phys. Rev. **5**, 2217 (1972).
 [21] G.E. Notkin, S.G. Rautian, and A.A. Feoktistov, Zh. Éksp. Teor. Fiz. **52**, 1673 (1967) [Sov. Phys. JETP **25**, 1112 (1967)].
 [22] M.S. Feld and A. Javan, Phys. Rev. **177**, 540 (1969).

- [23] Th. Hänsch and P. Toschek, *Z. Phys.* **236**, 213 (1970).
- [24] E.V. Baklanov and V.P. Chebotaev, *Zh. Éksp. Teor. Fiz.* **60**, 552 (1971) [*Sov. Phys. JETP* **33**, 300 (1971)].
- [25] S. Haroche and F. Hartmann, *Phys. Rev.* **6**, 1280 (1972).
- [26] Th. Hänsch and P. Toschek, *IEEE J. Quantum Electron.* **QE-4**, 467 (1968).
- [27] Th. Hänsch, R. Keil, A. Schabert, Ch. Schmelzer, and P. Toschek, *Z. Phys.* **226**, 293 (1969).
- [28] G.I. Topygina and É.E. Fradkin, *Zh. Éksp. Teor. Fiz.* **82**, 429 (1982) [*Sov. Phys. JETP* **55**, 246 (1982)].
- [29] R.W. Boyd and S. Mukamel, *Phys. Rev. A* **29**, 1973 (1984).
- [30] M. Sargent III, *J. Opt. Soc. Am. B* **5**, 987 (1988).
- [31] D.A. Holm, M. Sargent III, and L.M. Hoffer, *Phys. Rev. A* **32**, 963 (1985).
- [32] G. Khitrova, P. Berman, and M. Sargent III, *J. Opt. Soc. Am. B* **5**, 160 (1988).
- [33] R.W. Boyd, and M. Sargent III, *J. Opt. Soc. Am. B* **5**, 99 (1988).
- [34] M.T. Gruneisen, K.R. MacDonald, and R.W. Boyd, *J. Opt. Soc. Am. B* **5**, 123 (1988).
- [35] B.A. Capron, A.S. Marathay, and M. Sargent III, *Opt. Lett.* **11**, 70 (1986).
- [36] B.A. Capron and M. Sargent III, *Phys. Rev. A* **34**, 3034 (1986).
- [37] G. Grynberg, M. Vallet, and M. Pinard, *Phys. Rev. Lett.* **65**, 701 (1990).
- [38] M. Pinard, R.W. Boyd, and G. Grynberg, *Phys. Rev. A* **49**, 1326 (1994).
- [39] J. Guo, P.R. Berman, B. Dubetsky, and G. Grynberg, *Phys. Rev. A* **46**, 1426 (1992).
- [40] P.R. Berman, B. Dubetsky, and J. Guo, *Phys. Rev. A* **51**, 3947 (1995).
- [41] J.-Y. Courtois, G. Grynberg, B. Lounis, and P. Verkerk, *Phys. Rev. Lett.* **72**, 3017 (1994).
- [42] D. Marcuse, *Proc. IEEE* **1**, 849 (1963).
- [43] H.K. Holt, *Phys. Rev. A* **6**, 1136 (1977).
- [44] L.A. Rivlin, *Kvant. Electron. (Moscow)* **9**, 513 (1992) [*Sov. J. Quantum Electron.* **22**, 471 (1992).]
- [45] N.P. Bigelow and M.G. Prentiss, *Phys. Rev. Lett.* **65**, 555 (1990).
- [46] J.J. Tollett, J. Chen, J.G. Story, N.W.M. Ritchie, C.C. Bradley, and R.G. Hulet, *Phys. Rev. Lett.* **65**, 559 (1990).
- [47] E. Kyrölä and S. Stenholm, *Opt. Commun.* **22**, 123 (1977).
- [48] A.P. Kazantsev, *Sov. Phys. Usp.* **21**, 58 (1978).
- [49] V.S. Letokhov and V.G. Minogin, *Phys. Rep.* **73**, 1 (1981).
- [50] A.P. Kazantsev, V.S. Smirnov, G.I. Surdutovich, D.O. Chudesnikov, and V.P. Yakovlev, *J. Opt. Soc. Am. B* **2**, 1731 (1985).
- [51] J. Dalibard and C. Cohen-Tannoudji, *J. Opt. Soc. Am. B* **2**, 1707 (1985).
- [52] V.G. Minogin and O.T. Serimaa, *Opt. Commun.* **30**, 373 (1979).
- [53] R. Bonifacio, L. De Salvo, L.M. Narducci, and E.J. D'Angelo, *Phys. Rev. A* **50**, 1716 (1994).
- [54] M. Perrin, G.L. Lippi, and A. Politi, *Phys. Rev. Lett.* **86**, 4520 (2001).
- [55] M. Perrin, G.L. Lippi, and A. Politi, *J. Mod. Opt.* **49**, 419 (2002).
- [56] W.J. Brown, J.R. Gardner, D.J. Gauthier, and R. Vilaseca, *Phys. Rev. A* **55**, R1601 (1997).
- [57] W.J. Brown, J.R. Gardner, D.J. Gauthier, and R. Vilaseca, *Phys. Rev. A* **56**, 3255 (1997).
- [58] G.L. Lippi, G.P. Barozzi, S. Barbay, and J.R. Tredicce, *Phys. Rev. Lett.* **76**, 2452 (1996).
- [59] P.R. Hemmer, N.P. Bigelow, D.P. Katz, M.S. Shahriar, L. De Salvo, and R. Bonifacio, *Phys. Rev. Lett.* **77**, 1468 (1996).
- [60] S. Barbay, G. Fabre, and G.L. Lippi, *Opt. Commun.* **165**, 119 (1999).
- [61] M.G. Prentiss and S. Ezekiel, *Phys. Rev. Lett.* **56**, 46 (1986).
- [62] M.G. Prentiss and S. Ezekiel, *Phys. Rev. A* **35**, 922 (1987).
- [63] W.W. Quivers, Jr., *Phys. Rev. A* **34**, 3822 (1986).
- [64] S. Singh and G.S. Agarwal, *Phys. Rev. A* **42**, 3070 (1990).
- [65] W. Happer, *Rev. Mod. Phys.* **44**, 169 (1972).
- [66] B.R. Mollow, *Phys. Rev.* **2**, 76 (1970).
- [67] D. Grandclément, G. Grynberg, and M. Pinard, *Phys. Rev. Lett.* **59**, 40 (1987).
- [68] P.R. Berman, P.F. Liao, and J.E. Bjorkholm, *Phys. Rev. A* **20**, 2389 (1979).
- [69] R.A. MacDonald and D.H. Tsai, *Phys. Rep.* **6**, 1 (1978).
- [70] R.G. Brown and M. Ciftan, *Phys. Rev. A* **40**, 3080 (1989).
- [71] We remark that the approximation adopted in Ref. [53], where the averages of the products containing the atomic momentum and its polarization are done separately—as is commonly done also for the field-polarization terms—is certainly not a cause of concern for the regime of parameters which we explore in this paper. Indeed, we are interested in investigating the situation where collisions occur fairly infrequently and where the time scales over which momentum and polarization are very different (cf. later in this section, in particular, Fig. 1). Thus, we can consider the momentum constant over the typical response time of the atomic polarization and factor the averages.
- [72] We have tested the effect of collisions between bodies of different masses (i.e., collisions where imperfect transfer of energy and momentum takes place). Preliminary numerical runs show that, aside from quantitative modifications, the physics of the observed phenomena (the phase transition) remains unaltered.
- [73] B.R. Mollow, *Phys. Rev.* **188**, 1969 (1969).
- [74] This statement is basically equivalent to assuming that no density grating is to be expected. While this holds true in the parameter region investigated in this paper, we do not rule out the possibility that such a grating may arise for sufficiently large pump intensities or at sufficiently low temperatures.
- [75] M. Perrin, Z. Ye, and L.M. Narducci, *Phys. Rev. A* **66**, 043809 (2002).
- [76] A.E. Siegman, *Lasers* (University Science Books, Mills Valley, CA, 1986).